

Specific heat of $\text{Zr}_{65}\text{Al}_{7.5}\text{Cu}_{17.5}\text{Ni}_{10}$ around the glass transition

 B. Reinker^a, M. Dopfer, M. Moske, and K. Samwer

Institut für Physik, Universität Augsburg, Universitätsstrasse 1, 86135 Augsburg, Germany

Received: 23 January 1998 / Received in final form and Accepted: 31 August 1998

Abstract. Dynamic calorimetric measurements are performed for the quaternary metallic glass $\text{Zr}_{65}\text{Al}_{7.5}\text{Cu}_{17.5}\text{Ni}_{10}$ in order to analyse the dependence on different heating rates for the glass transition temperature T_g . We compare two different temperature programs used for sample relaxation, to estimate the influence of the thermal history on T_g . A lower limit for the glass transition temperature T_g was calculated according to two different models based on the fact, that width and temperature of the glass transition depend on the experimental time scale set by the heating rate: One model assumes a Vogel-Fulcher-Tammann type behaviour, as used to describe more or less “fragile” glass formers and the other assumes an Arrhenius-like behaviour, which is related to “strong” glass formers. The values obtained from both models differ by about 80K. From additional absolute specific heat capacity measurements we calculate the Kauzmann temperature T_K , as a lower limit for the temperature of the glass transition from thermodynamic aspects. Comparing T_K with the temperature values obtained from the two evaluation models we can classify the quaternary metallic glass $\text{Zr}_{65}\text{Al}_{7.5}\text{Cu}_{17.5}\text{Ni}_{10}$, to behave more like a “strong” glass former.

PACS. 81.05.Kf Glasses (including metallic glasses) – 64.70.Pf Glass transitions – 81.70.Pg Thermal analysis, differential thermal analysis (DTA), differential thermogravimetric analysis

1 Introduction

Recently new metallic glasses were found which exhibit a distinct glass transition combined with a wide super cooled liquid region [1, 2]. The quaternary so-called Inoue-alloy of composition $\text{Zr}_{65}\text{Al}_{7.5}\text{Cu}_{17.5}\text{Ni}_{10}$ offers a temperature range of about 127 K between glass transition T_g and crystallization temperature T_x for the highest heating rates used [3]. Due to the high thermal stability of the undercooled liquid against crystallization, this special alloy is favorite for a detailed study of the thermophysical properties of the undercooled melt. Furthermore, in contrast to most conventional glass formers, the glass transition can be investigated in a wide range of time scales. In this paper we focus on the dynamic aspects of the glass transition as well as on thermodynamics with respect to Differential Scanning Calorimetry (DSC) measurements. From dynamic measurements we obtain the glass transition temperature, which varies with the chosen heating rate. However, since T_g depends on the thermal history of the sample, we first have to define a reference state for all measurements. We used two different methods to relax our samples. For the first series as prepared samples have been used for which the initial state is related to the heating rate used during the DSC scan and for the second method the initial state is the same for all samples. Our aim is on one hand to find a capable method

for quantitative comparisons on T_g and on the other hand to determine a lower limit for the glass transition temperature. From measurements of the absolute specific heat capacity the thermodynamic quantities are calculated as a function of temperature. Thus, we are able to calculate the Kauzmann temperature T_K , which represents a lower limit for the kinetically observed glass transition from thermodynamic aspects [4].

2 Experimental methods

$\text{Zr}_{65}\text{Al}_{7.5}\text{Cu}_{17.5}\text{Ni}_{10}$ ingots were prepared by arc-melting a mixture of pure Zr, Al, Cu and Ni in an argon atmosphere (4N8). From the master alloy we prepared pellets of about 100–120 mg. Using ultra-rapid quenching we obtained splats with thickness of 45–50 μm and of about 2.5 cm in diameter. The amorphous state of the splats was verified by X-ray diffraction. Pieces of 6 mm in diameter and typically 20–40 mg were punched out from the splats. The heatflow of the samples is measured in a modified Perkin Elmer DSC7 at constant gas-pressure, using Al-pans with holes. During the experiment the DSC-head was purged with dry argon gas (4N8) at a flow of about 30 ml/min.

Prior to the experiments the samples were relaxed in the DSC, to allow irreversible structural relaxation of the quenched in excess free volume. We applied two different relaxation methods. By using *method 1*, each sample was

^a e-mail: bernward.reinker@physik.uni-augsburg.de

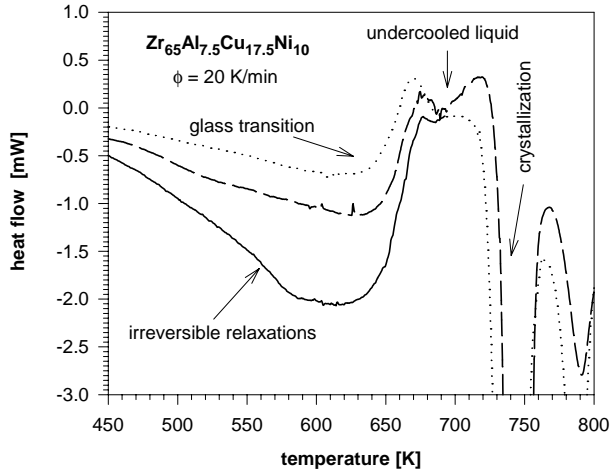


Fig. 1. Comparison of the DSC thermograms of an as quenched sample (solid line) and of samples treated with two different measurement methods, *method 1* (dotted line) and *method 2* (dashed line) as described in the text.

first heated above the glass transition temperature T_g into the metastable region of the undercooled liquid with a rate ϕ and then cooled down to the starting temperature using the same rate. Subsequently, the heatflow curve was then measured again with the same heating rate ϕ . Since the cooling rate and the heating rate are the same the evolution of the sample is tested only on a single time scale corresponding to the chosen rate ϕ . For investigations carried out with the *method 2* each sample was first heated above T_g with a rate of 20 K/min and then cooled down to the starting temperature with a rate of 200 K/min. Thus, the initial state for these samples is always the same. The measurement then was performed with an individual heating rate ϕ_i for each sample. At the end of the measurement the samples were crystallized and an additional DSC scan was recorded at the same measuring conditions for direct comparison.

For the specific heat capacity evaluation we have measured the static heat flow at distinct temperature levels. The amorphous samples are analyzed up to 720 K and the crystallized samples up to 893 K. Using a high temperature calorimeter of type SETARAM we obtained the values of c_p far above the melting point T_m . The experiments were performed in the so-called “step-mode”. Therefore, the relaxed sample (*method 2*) was first heated with $\phi = 10$ K/min to a specified temperature, followed by an isothermal step for 180 s. The resulting step change in heat flux is then compared with the signal of a sapphire standard (Al_2O_3). This procedure was repeated in intervals of 10 and 20 K.

3 Results

The glass transition for the amorphous $\text{Zr}_{65}\text{Al}_{7.5}\text{Cu}_{17.5}\text{Ni}_{10}$ -alloy was investigated in DSC experiments for a variety of heating rates for the two methods of preannealing mentioned above. Figure 1 shows the DSC thermogram of two $\text{Zr}_{65}\text{Al}_{7.5}\text{Cu}_{17.5}\text{Ni}_{10}$ -samples, one is relaxed with *method 1* and one with *method 2*, in comparison with an *as quenched* specimen. The amount of free volume reduction, as indicated by the irreversible changes in the heatflow below T_g , is higher for those samples preprocessed with *method 1*. In Figure 2 the heatflow curves throughout the glass transition, depending on different heating rates, are presented for both methods. The signal-to-noise ratio for the second series (*method 2*) is increased stronger with decreasing heating rate, as compared with those samples which are relaxed by *method 1*. Consequently, it is impossible for the measurements shown to exactly determine the T_g values for heating rates smaller than 1 K/min.

From static measurements the absolute specific heat capacity c_p is calculated with respect to a sapphire standard. Starting with the enthalpy change $dQ = c_p m dT$, of a sample with mass m the derivation in time leads to the following expression:

$$\frac{dQ}{dt} = c_p m \frac{dT}{dt}. \quad (1)$$

dQ/dt represents the heatflow signal H and dT/dt is equal to the heating rate ϕ . It is important to note, that in DSC experiments only part of the heatflow is used to heat up the sample to a certain temperature ($dT/dt \neq 0$) whereas another part compensates the constant flow of the cooling gas, within the isothermal interval ($dT/dt = 0$). Therefore, neglecting further time dependent isothermal effects equation (1) has to be extended to

$$\left(\frac{dQ}{dt}\right)_{\dot{T} \neq 0} - \left(\frac{dQ}{dt}\right)_{\dot{T} = 0} = \Delta H = c_p m \frac{dT}{dt}. \quad (2)$$

The left side of equation (2) equals the difference in heatflow signal from the beginning and the end of the isothermal step. In order to exclude instrumental errors, the heat capacity measurements are evaluated relative to a sapphire standard, with the pure Al-pan signal subtracted first. One then obtains the following expression for the molar specific heat capacity of the sample

see equation (3) below.

M_{sample} and M_{sapphire} are the molar masses of the sample and the sapphire standard respectively. It should be remarked, that constant and well defined experimental conditions are absolutely necessary for the calculation of c_p .

$$c_{p \text{ sample}}(T) = \frac{(\Delta H_{\text{sample}}(T) - \Delta H_{\text{empty}}(T)) m_{\text{sapphire}} M_{\text{sample}}}{(\Delta H_{\text{sapphire}}(T) - \Delta H_{\text{empty}}(T)) m_{\text{sample}} M_{\text{sapphire}}} c_{p \text{ sapphire}}(T) \quad (3)$$

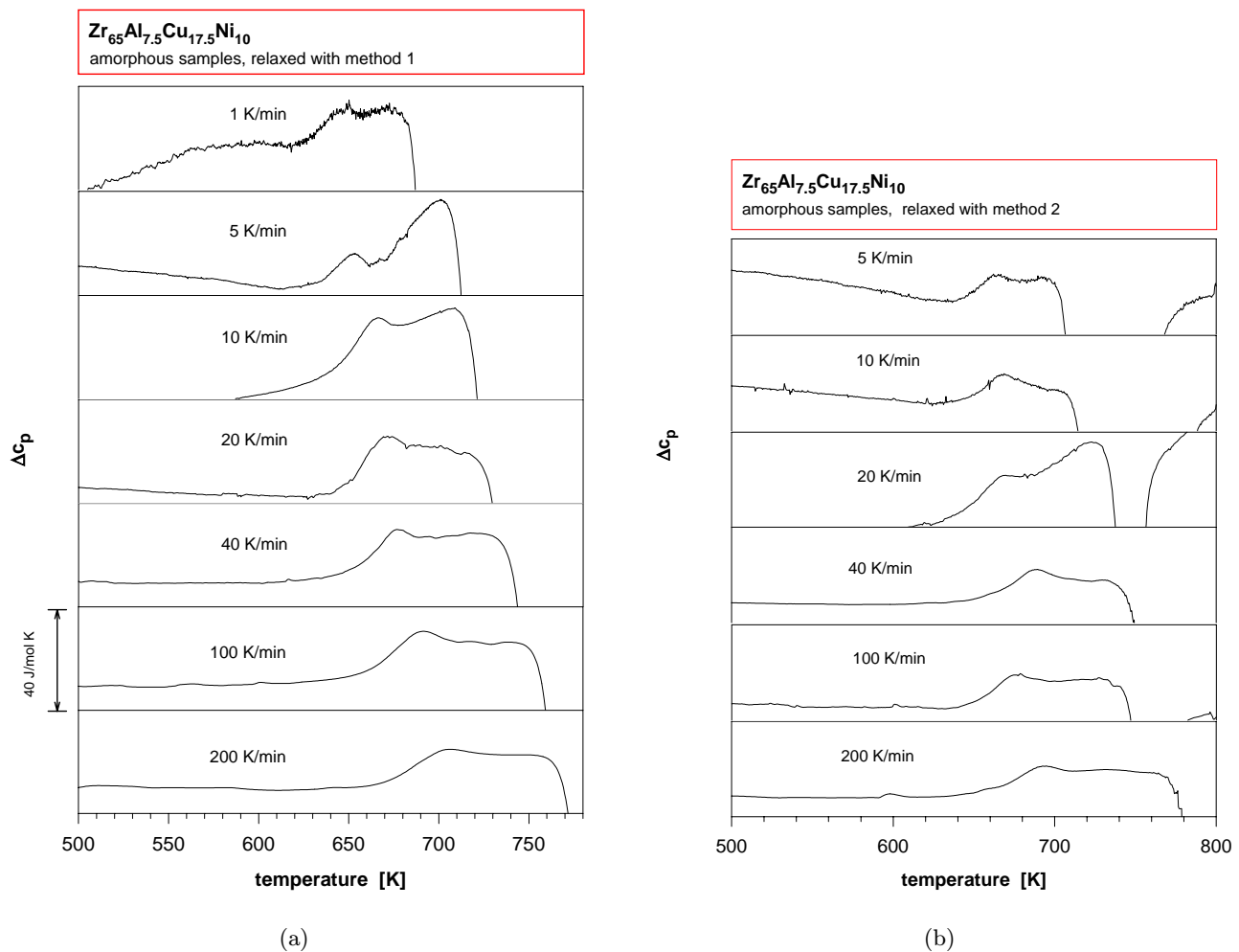


Fig. 2. The specific heat capacities Δc_p of the samples relative to the crystalline reference for heating rates of 1 K/min to 200 K/min using (a) *method 1* and (b) *method 2*.

For the c_p calculations of the amorphous and the crystalline $Zr_{65}Al_{7.5}Cu_{17.5}Ni_{10}$ we need additional information about the melting point T_m and the enthalpy of fusion H_m , which can be obtained from high temperature DSC measurements. In Figure 3 the complete DSC-run is presented, including the heating and cooling cycle. The shaded area is the enthalpy of fusion which is used for further calculations.

4 Discussion

From DSC experiments the glass transition temperatures are determined. Due to the effect of delayed relaxation in dynamic measurements, the glass transition has a finite width ΔT [5]. According to Figure 4 we use the temperature interval between the values of T_g -onset and T_g -end. Based on these data we have calculated the lower limit for the glass transition. Assuming a Vogel-Fulcher-Tammann (VFT) type behaviour for the glass transition as proposed

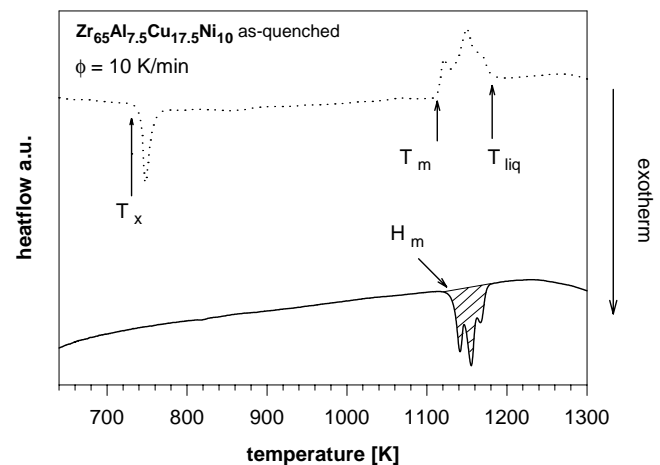


Fig. 3. DSC run, heating (dotted line) and cooling (solid line), performed in the high temperature DSC of type SETARAM. The melting point $T_m = 1107$ K and the enthalpy of fusion $H_m = 7245.6$ J/mol are marked, which were used for further thermodynamic calculations.

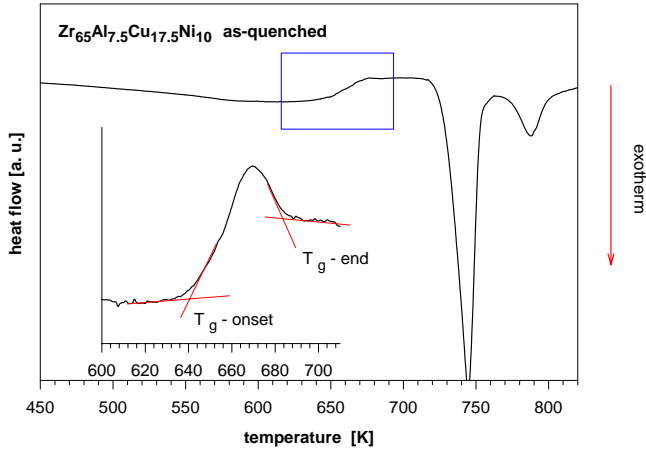


Fig. 4. Illustration for the definition of the used T_g -onset end T_g -end temperatures.

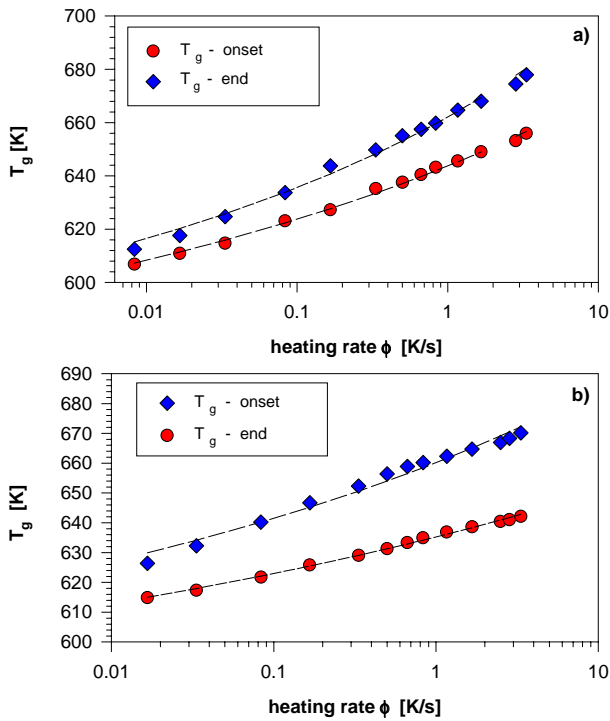


Fig. 5. T_g -onset and T_g -end values versus heating rate for (a) *method 1* and (b) *method 2* with the fits included, assuming a VFT like behaviour.

by R. Brüning *et al.* [6], one can calculate a lower limit T_g^I by using the following expression:

$$\phi = B \exp \left\{ \frac{A}{T_g^I - T_g} \right\} \Leftrightarrow T_g = T_g^I + \frac{A}{\ln\{B/\phi\}}. \quad (4)$$

The temperature T_g^I is the asymptotic value of T_g in the limits of infinitely slow cooling or heating rates. The parameter B has the dimension of a heating rate. Figure 5 shows the data with the best fits (*dashed lines*) for both temperature programs.

With decreasing heating rate T_g -onset and T_g -end converge to the same value within a range of ± 3 K, *i.e.*, in

Table 1. Calculated lower limits for the glass transition of $Zr_{65}Al_{7.5}Cu_{17.5}Ni_{10}$.

critical temperature	measurement method	value of method 1	value of method 2
T_g^I	dynamic	509 ± 3 K	512 ± 3 K
T_g^{II}	dynamic	589 ± 5 K	590 ± 5 K
T_K	calorimetric	–	598 ± 10 K

the limit of infinitely slow heating and cooling rate the heatflow should become a step function at the glass transition. Furthermore, for the two relaxation methods the calculated temperatures T_g^I differ only by about 2 K. The obtained values are presented in Table 1. Considering the experimental uncertainties, T_g^I is independent of the thermal history.

However, if one assumes an Arrhenius-like behaviour, which corresponds to the VFT formula in the limit of $T_g^I \rightarrow 0$, the dependence between T_g and heating rate is written as [7]

$$T_g = \frac{A'}{\ln\{B'/\phi\}}, \quad (5)$$

with A' proportional to an activation energy. In this context the width of the glass transition ΔT is an important parameter, which contains the time dependent effects of the sample. With slower heating rates a narrowing of the transition range is observed, which can be expressed by [7]

$$\frac{\Delta T}{T_g} \propto \frac{1}{\ln\{B'/\phi\}}. \quad (6)$$

Combining equations (5, 6) we obtain the following relation

$$\Delta T \propto \frac{1}{A'} (T_g)^2. \quad (7)$$

The lower limit for the glass transition T_g^{II} is obtained by extrapolating the regression curve to $\Delta T = 0$, as shown in Figure 6. The value for T_g^{II} is about 590 ± 5 K and is independent of the relaxation method used, within the experimental uncertainties. However, the activation energy, as indicated by the slope of the fits, is higher for *method 1*.

Comparing the two different evaluation models, we find that the lower limit values of T_g differ by about 80 K. Thus, we have applied a third method to calculate the lower limit of the glass transition from measurements of the absolute specific heat capacity. In Figure 7 the measured values of c_p for the crystalline and amorphous state are shown. According to Kubaschewski *et al.* [8] the temperature dependence of the specific heat capacity in the undercooled liquid can be expressed mainly as a T^{-2} -law:

$$c_{pl} = 3R + bT + cT^{-2}. \quad (8)$$

The fits according to equation (8) for both, the crystal and the undercooled liquid, are included in Figure 7. Since

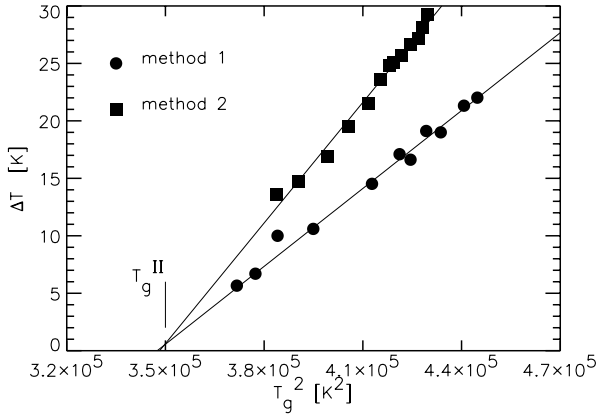


Fig. 6. ΔT versus T_g^{II} (see Eq. (7)). In the limit $\Delta T \rightarrow 0$ we observe T_g^{II} .

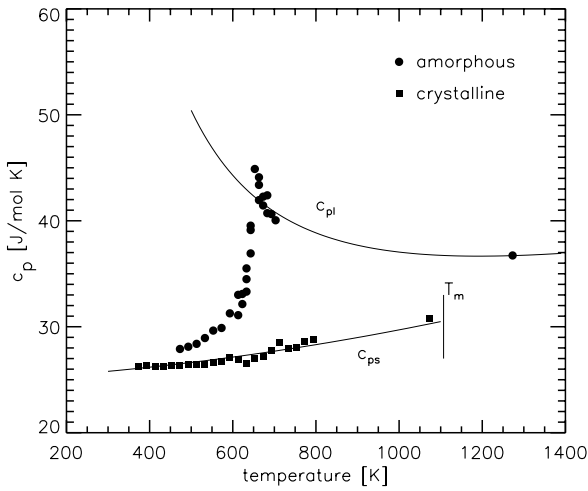


Fig. 7. The absolute specific heat capacity of $\text{Zr}_{65}\text{Al}_{7.5}\text{Cu}_{17.5}\text{Ni}_{10}$ for the crystalline, the amorphous, and the liquid state. The lines show the best fit to the data according to Kubaschewski *et al.* [8]. The c_p -value in the melt was obtained with a high temperature DSC (SETARAM).

the temperature dependence of the specific heat capacity in the $\text{Zr}_{65}\text{Al}_{7.5}\text{Cu}_{17.5}\text{Ni}_{10}$ -alloy is known for the non-crystalline and the crystalline state as well, the excess entropy ΔS with respect to the crystal can be calculated by

$$\Delta S = \frac{H_m}{T_m} - \int_T^{T_m} [c_{pl} - c_{ps}] \frac{dT'}{T'}, \quad (9)$$

with c_{pl} and c_{ps} as determined for the specific heat capacity of the liquid and the the crystalline state, respectively. Figure 8 shows this calculated entropy difference. The entropy of the melt decreases with increasing undercooling, until it reaches the entropy of the crystal at the Kauzmann temperature T_K . The existence of an undercooled liquid below this temperature would violate thermodynamic rules, also called the Kauzmann paradox.

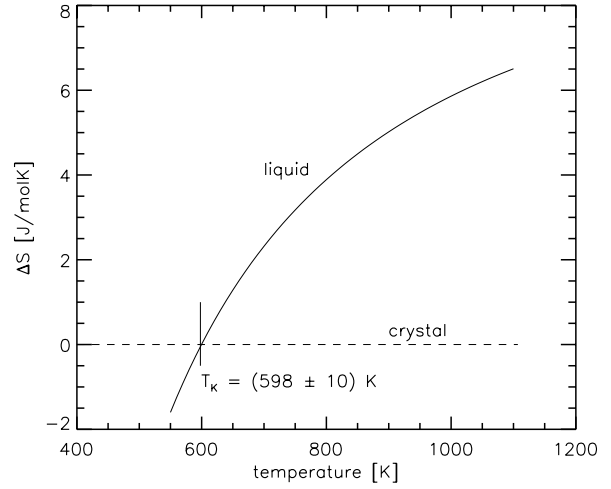


Fig. 8. The excess entropy ΔS of the liquid state with respect to the crystal. $T_{\Delta S=0}$ is the so-called Kauzmann temperature T_K .

Therefore, T_K will be the lower boundary for the glass transition from thermodynamic aspects. For our system we obtain a Kauzmann temperature T_K of 598 ± 10 K.

Table 1 gives an overview of the critical temperatures for the glass transition, as calculated from the different models. The value of T_g^I obtained from the VFT type functional differs by about 80 K from the other ones. In contrast, the value of T_g^{II} is very close to the calculated Kauzmann temperature T_K . This seems to be a common feature for this special type of metallic glasses. $\text{Zr}_{46.5}\text{Ti}_{8.25}\text{Cu}_{7.5}\text{Ni}_{10}\text{Be}_{27.5}$ for instance shows a similar behaviour for the shear viscosity fitted to the empirical VFT-equation, the calculated VFT-temperature is about 150K below T_K [9]. From other experiments it is known that the diffusion coefficient in $\text{Zr}_{65}\text{Al}_{7.5}\text{Cu}_{17.5}\text{Ni}_{10}$ as well as in ZrTiCuNiBe-alloys do not change as dramatically as one would expect, if the Vogel-Fulcher equation was valid [10]. From the fact, that an Arrhenius type behaviour in its thermodynamic limit leads to a glass transition temperature equal to the Kauzmann temperature, we can classify $\text{Zr}_{65}\text{Al}_{7.5}\text{Cu}_{17.5}\text{Ni}_{10}$, to behave more like a “strong” glass former. This agrees with the classification using the fragility index [11]

$$m = \left. \frac{d(\log \eta)}{d(T_g/T)} \right|_{T=T_g}, \quad (10)$$

which is determined from the temperature dependence of the shear viscosity $\eta(T)$ at the glass transition temperature T_g . Values obtained for glass forming systems based on ZrAlCu are $m = 36.4$ for $\text{Zr}_{65}\text{Al}_{7.5}\text{Cu}_{27.5}$ [12] and $m = 46.1$ for $\text{Zr}_{65}\text{Al}_{7.5}\text{Cu}_{17.5}\text{Ni}_{10}$ (estimated from Ref. [13]). These values are close to the strong coupled systems SiO_2 and GeO_2 with a fragility index of 20 [11].

Let us now focus on the two different relaxation methods used. The main difference between the two methods

arises from the fact, that for the *method 2* the metastable state of the undercooled liquid is partly frozen, due to the fast cooling at 200 K/min. This can easily be seen in Figure 1, where the irreversible volume relaxation for the samples preprocessed with the *method 2* is smaller than for those treated with the *method 1*. Comparing the determined lower boundaries for the glass transition temperatures of the metallic glass $Zr_{65}Al_{7.5}Cu_{17.5}Ni_{10}$, one obtains identical values for the two different methods of relaxation applied. If we consider, that the glass transition temperature obtained in the limit of infinitely slow relaxation kinetics (*i.e.*, infinitely small heating rates) is equivalent with the thermodynamic equilibrium value of the transition, there are no further effects expected depending on preparation conditions or on the thermal history of the sample. This is confirmed by our measurements. The two relaxation methods only affect the activation energies for the relaxation process, as indicated by the two different slopes for the fits in Figure 6.

5 Conclusion

Dynamic calorimetric measurements of the glass transition, extended to low heating rates, and measurements of the absolute specific heat capacity under isothermal conditions are performed for the amorphous $Zr_{65}Al_{7.5}Cu_{17.5}Ni_{10}$ -alloy. From the static measurements the Kauzmann temperature T_K was determined which represents the lower boundary of glass transition temperature. In addition, two different models were used to describe the heating rate dependence of the obtained T_g -data and to calculate a lower limit of the glass transition temperature from dynamic measurements. The T_g^I -value obtained by a Vogel-Fulcher-Tammann like dependence of the heating rate is far below the Kauzmann temperature, while an Arrhenius-type behaviour in connection with the extended free volume model, gives a lower limit T_g^{II} close to T_K . The second model is related to the more "strong" glass formers. Thus, we classify amorphous $Zr_{65}Al_{7.5}Cu_{17.5}Ni_{10}$ to belong to this kind of glasses

too, based on a Zr-network acting as a backbone to the system. Although two different methods were used to allow irreversible structural relaxation in a preanneal, the obtained lower limits are nearly the same for both measurement methods, *i.e.*, the obtained values for the lower glass temperature limit are independent of the thermal history within the parameters of measurement. However, comparing both methods of relaxation, the method which only tests one characteristic time scale, seems to be the appropriate one for quantitative investigations on the glass transition.

The authors would like to thank R. Brüning and F. Sommer for valuable discussions and M. Mertinat for the investigations carried out with the high temperature DSC of type SETARAM. Financial support by the DFG, *Schwerpunktprogramm: "Glasübergang"*, is gratefully acknowledged.

References

1. T. Masumoto, Sci. Rep. RITU A **39**, 91 (1994).
2. W.L. Johnson, NATO Adv. Stud. Inst. E **278**, 25 (1994).
3. A. Inoue, T. Zhang, T. Masumoto, J. Non-Cryst. Solids **156-158**, 473 (1993).
4. W. Kauzmann, Chem. Rev. **43**, 176 (1948).
5. J. Jäckle, Rep. Prog. Phys. **49**, 171 (1986).
6. R. Brüning, K. Samwer, Phys. Rev. B **46**, 11318 (1992).
7. J. Jäckle, J. Phys.-Cond. **1**, 267 (1989).
8. O. Kubaschewski, C.B. Alcock, P.J. Spencer, *Materials Thermochemistry*, 6th edn. (Pergamon Press, 1993).
9. R. Bush, E. Bakke, W.L. Johnson, Mat. Sci. For. **235-238**, 327 (1997).
10. U. Geyer, Phys. Rev. Lett. **75**, 2364 (1995).
11. R. Böhmer, C.A. Angell, in *Disorder Effects on Relaxational Processes*, edited by R. Richert, A. Blumen (Springer Verlag, Berlin, 1994).
12. R. Rambousky, M. Moske, K. Samwer, Z. Phys. B. **99**, 387 (1996).
13. W. Ulfert, H. Kronmüller, J. Phys. IV Colloq. France **6**, C6-617 (1996).